29th Congress of the International Council of the Aeronautical Sciences
St. Petersburg, Russia; September 7-12, 2014

USING A BIODYNAMIC MODEL TO INVESTIGATE THE EFFECTS OF BODY-BORNE EQUIPMENT ON FORCES EXPERIENCED IN A SIMULATED HELICOPTER CRASH

Daniel Aggromito[1,2], Rodney Thomson[2,3], John Wang[4] , Bernard Chen[1], Wenyi Yan[1]
[1]Department of Mechanical & Aerospace Engineering,
Monash University, Clayton Victoria 3800, Australia
[2]Cooperative Research Centre for Advanced Composite Structures,
1/320 Lorimer Street, Port Melbourne, Victoria, 3207, Australia
[3] Advanced Composite Structures Australia Pty Ltd,
1/320 Lorimer Street, Port Melbourne, Victoria, 3207, Australia
[4]Defence Science and Technology Organisation,
506 Lorimer Street, Fishermans Bend, Victoria, 3207, Australia

Keywords: Helicopter Crash, Crashworthiness, Injury, Body-Borne Equipment

Abstract

The effects of body-borne equipment on forces and accelerations experienced by occupants during a helicopter crash are investigated. Helicopter seats are designed to a specified weight range including equipment. Over recent years, occupants have been required to carry increasing amounts of equipment on their body, which may affect the probability of injury during a crash. In this study, the human body is represented as a four degree-of-freedom mass-spring-damper model. Equipment is attached at the hip, upper torso and head using springs and dampers and varied to investigate its effects. The proposed model with equipment attached is a 7-degree-of-freedom mass-spring-damper model. Equations are developed to replicate the energy absorption characteristics of a 'Fixed Load Energy Absorption' device used in crashworthy seats. The forces relating to injury criteria experienced during a helicopter crash were analysed using a simple numerical procedure with a transient analysis with sufficiently small time steps in MATLAB. The effects of initial impact velocity were investigated and the results demonstrated that the seat's ability to absorb the impact energy reduces with increased equipment mass at higher initial impact velocities. Furthermore, increased equipment mass has major consequences on the forces at the lumbar, upper torso and head.

1 Introduction

During a crash, a helicopter will experience large deceleration forces in the vertical, forward and lateral directions, which are substantial and have the high potential for causing injury to occupants if unprotected by crashworthy systems. A crashworthy seat is designed to absorb energy through a load limit mechanism. This mechanism allows the seat and occupant to move at loads just under humanly tolerable limit, over the maximum distance between the seat pan and the cabin floor [1]. The seat mechanism is designed for a specified range of occupant weight to provide limited protection by absorbing impact energy up to a specific maximum value.

Military-Standard-58095A [2] dictates that the seat be designed at the heavy end for an occupant that has a mass of 91 kg with 15 kg of equipment. Current body-borne equipment can exceed 30 kg depending on the type of mission. This may lead to a phenomenon called "bottom-out" in which the full stroking distance is reached before the impact energy is totally

absorbed, imparting a higher impact force than the humanly tolerable limit [3].

The simplest method to represent the human body is a lumped parameter model which considers the human body as several concentrated masses connected by springs and dampers. A number of models have been developed ranging from one–degree-of-freedom (DOF) to multi-DOF. A four-DOF model was developed by Wan & Schimmels [4] in which the human body was segregated into four mass-bodies, the lower torso, upper torso, head and viscera. The parameters were selected by matching relevant available data from experimental tests. A literature survey on representing the human body using lumped parameter models was conducted by Liang & Chiang [5]. In this study, a number of models with varying DOFs were compared and validated against experimental data. The results illustrated that the model developed by Wan & Schimmels [4] produced the best results against a number of criteria including apparent mass, driving point mechanical impedance and seat to head transmissibility.

The effects of body-borne equipment on an occupant in a helicopter crash are uncertain and research relating to it is minimal. Richards & Sieveka [6] developed a model using the software MADYMO to investigate lumbar loads. They varied the equipment mass from 0 – 20 kg on an ellipsoid hybrid III Anthropomorphic Test Device (ATD). The results demonstrated a substantial increase in lumbar loads of 61%. However, the study only investigated equipment mass located at the upper torso and did not analyse the effect of attachment types on loading magnitudes.

In this paper, a four-DOF lumped parameter model used to represent the human body and the forces experienced by a seated occupant during a helicopter crash is examined. Equipment is attached at the hip, upper torso and head using springs and dampers. Equations are devised to represent the force control of a crashworthy seat utilizing a fixed load energy absorption device (FLEA). The model is solved using the Fourth-Order-Runge-Kutta method utilized by the ODE45 function in MATLAB. The influence of equipment mass and attachment types on forces on the lower torso, upper torso and head is analysed through varying the mass, spring and damping coefficients and simulated under an initial impact velocity to determine its effects.

2 Occupant Model with Equipment

2.1 Occupant Model

The occupant model is a four-DOF lumped parameter model that closely replicates that proposed by Wan & Schimmels [4], see Figure 1. The major difference between the models is the seat and lower torso is considered one mass body in the current study. The viscera is identified as one of the most important subsystems when excited in the sitting position as the abdominal mass vibrates in and out of the thoracic cage under the influence of longitudinal vibration. A spring and damper is used to represent the spinal column and connects the lower torso to the upper torso. The head is its own mass body and is connected to the upper torso by a spring and damper.

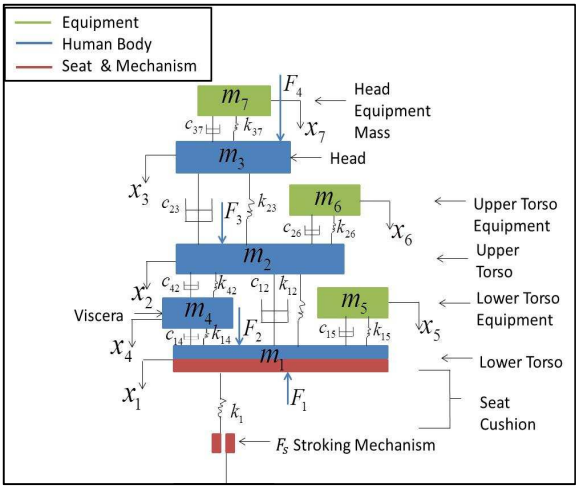

Figure.1. The occupant model with equipment attached demonstrating locations of force measured.

The mass, spring and damping parameters were taken from the models proposed by Payne & Band [7] and Wan & Schimmels [4]. The values are not identical to these two models. An average value of each of the spring and damping coefficients of the models was utilised. It was found that these models had very similar values for the mass,

spring and damping parameters. Furthermore, the difference in values between the two models had an inconsequential effect on the forces measured as a result of increased equipment [4][7]. The occupant has an effective mass of 62.5 kg and the model parameters are presented in T able 1.

Table 1: Occupant model parameters

Item	Location	Value
m_1 (kg)	Lower Torso	35
m_2 (kg)	Upper Torso	17.5
m_3 (kg)	Head	4.5
m_4 (kg)	Viscera	5.5
k_{12} (kN/m)	Lower Torso – Upper Torso	150
k_{14} (kN/m)	Lower Torso – Viscera	2
k_{23} (kN/m)	Upper Torso – Head and Neck	160
k_{42} (kN/m)	Viscera-Upper Torso	12.5
c_{12} (kN-s/m)	Lower Torso – Upper Torso	.81
c_{14} (kN-s/m)	Lower Torso – Viscera	.05
c_{23} (kN-s/m)	Upper Torso – Head and Neck	.424
c_{42} (kN-s/m)	Viscera – Upper Torso	.131

2.2 Equipment

Three equipment masses are attached at the lower torso, upper torso and head to mimic the location of equipment in real life military operations. To determine the effects of mass and increasing mass, the equipment mass varies from 10 kg to 40 kg at the lower torso and upper torso, and the head equipment mass ranges from 0.5 kg – 2 kg to represent a helmet with and without night vision goggles and counter. The equipment at the lower torso and upper torso includes everything considered fundamental to military operations and a list of equipment is displayed in table 2. It should be noted that this is not a comprehensive list of equipment, but aims to illustrate some of the equipment used by military aviators today [6]. Equipment can include chemical and biological gear depending on mission type (not listed in table 2), which substantially increases the equipment mass. The equipment masses are represented by m_5, m_6 and m_7 in Figure 1.

Table 2: A representation of the equipment worn by a U.S. Navy Rotorcraft Aviator size XL clothing and equipment [6]

Item	Mass (kg)
Helmet with Visor and Intercom	2.19
Night Vision Goggles	0.52
Flight Suit	1.02
Gloves	0.09
Survival Vest	1.96
Hoisting Harness	1.23
Flotation Collar	1.39
Radio	0.92
Air Bottle	1.09
Medical Kit + Supplies	0.99
Other Survival Gear	0.75
Hard Body Armour (two plates)	6.43
Miscellaneous Gear (Water, Weapon, Ammunition)	2.27
Total	20.84

2.3 Equipment Attachments

Each equipment mass is attached to the occupant with a spring and damper. To investigate the effects of attachment types on loading magnitudes, the stiffness coefficient is varied from loose attachment to tight attachment to consider the diverse equipment types ranging from body armour with tight attachment to hand guns with loose attachment. A loose attachment at the hip and upper torso is represented by a low stiffness coefficient (30 kN/m), semi-tight equipment attachment by a medium stiffness coefficient (60 kN/m) and tight equipment attachment by a high stiffness coefficient (90 kN/m). The values are chosen as an arbitrary guide to simulate the diverse attachment types. The stiffness coefficient used for the head equipment attachment, which represents the foam helmet liner was estimated by:

$$k = \frac{EA}{L} \tag{1}$$

where E is the Young's modulus; A is the cross-sectional area of the helmet liner and L is the length of the liner

Eq. (1) utilises the elastic modulus to calculate the axial stiffness of an element in tension or compression [8]. The Young's modulus of a representative foam was measured at 625 kPa using the elastic section of the stress-strain graph [9].

The damping coefficient for all equipment attachments was estimated by:

$$\zeta = \frac{c}{\sqrt{mk}} \tag{2}$$

where ζ is the damping ratio; m is the mass of the respective body and k is the stiffness coefficient.

A sensitivity analysis was used to determine the effects of the damping ratio. An underdamped condition of 0.1 and 0.5 and a critically damped condition of 1 were the damping ratios investigated. The maximum forces were found to be within 3% of each other, and therefore an underdamped condition of 0.5 was used. Table 3 shows the area, length and the corresponding spring coefficient of the helmet.

Table 3: Area and length of helmet liner and spring coefficient to represent the attachment of each condition.

Attachment Type	Area (m^2)	Length (m)	Spring Coefficient (kN/m)
Loose	0.0019	0.31	3.97
Semi-tight	0.066	0.34	6.03
Tight	0.145	0.38	10

2.4 Equations of motion

For the model, the equations of motion of the masses are governed by a set of differential equations that can be written in the general matrix form

$$\boldsymbol{M}\ddot{X} + \boldsymbol{C}\dot{X} + \boldsymbol{K}X = \boldsymbol{F} \tag{3}$$

where **M, C** and **K** are the mass, the damping coefficient and the stiffness coefficient matrices respectively.

$$\boldsymbol{M} = \begin{bmatrix} m_1 & 0 & 0 & 0 & 0 & 0 & 0 \\ 0 & m_2 & 0 & 0 & 0 & 0 & 0 \\ 0 & 0 & m_3 & 0 & 0 & 0 & 0 \\ 0 & 0 & 0 & m_4 & 0 & 0 & 0 \\ 0 & 0 & 0 & 0 & m_5 & 0 & 0 \\ 0 & 0 & 0 & 0 & 0 & m_6 & 0 \\ 0 & 0 & 0 & 0 & 0 & 0 & m_7 \end{bmatrix}$$

$$\boldsymbol{C} = \begin{bmatrix} c_{14} + c_{12} + c_{12} & -c_{12} & 0 \\ -c_{12} & c_{42} + c_{12} + c_{23} + c_{26} & -c_{23} \\ 0 & -c_{23} & c_{23} - c_{37} \\ -c_{14} & -c_{42} & 0 \\ -c_{15} & 0 & 0 \\ 0 & -c_{26} & 0 \\ 0 & 0 & -c_{37} \end{bmatrix}$$

$$\begin{bmatrix} -c_{14} & -c_{15} & 0 & 0 \\ -c_{42} & 0 & -c_{26} & 0 \\ 0 & 0 & 0 & c_{37} \\ c_{14} + c_{42} & 0 & 0 & 0 \\ 0 & c_{15} & 0 & 0 \\ 0 & 0 & c_{26} & 0 \\ 0 & 0 & 0 & c_{37} \end{bmatrix}$$

and

$$\boldsymbol{K} = \begin{bmatrix} k_{14} + k_{12} + k_{15} & -k_{12} & 0 \\ -k_{12} & k_{42} + k_{12} + k_{23} + K_{26} & -k_{23} \\ \mathbf{0} & -k_{23} & k_{23} - k_{37} \\ -k_{14} & -k_{42} & 0 \\ -k_{15} & 0 & 0 \\ 0 & -k_{26} & 0 \\ 0 & 0 & -k_{37} \end{bmatrix}$$

$$\begin{bmatrix} -k_{14} & -k_{15} & 0 & 0 \\ -k_{42} & 0 & -k_{26} & 0 \\ 0 & 0 & 0 & k_{37} \\ k_{14} + k_{42} & 0 & 0 & 0 \\ 0 & k_{15} & 0 & 0 \\ 0 & 0 & k_{26} & 0 \\ 0 & 0 & 0 & k_{37} \end{bmatrix}$$

$$\boldsymbol{F} = \begin{bmatrix} F_1 \\ 0 \\ 0 \\ 0 \\ 0 \\ 0 \\ 0 \end{bmatrix} \tag{4}$$

$X = [x_1\ x_2\ x_3\ x_4\ x_5\ x_6\ x_7]^T$ is a column vector containing the displacement of the 7 masses from Fig.1 from their equilibrium positions. These displacements are functions of time t and represent the freedom of the model. $\dot{\boldsymbol{X}}$ and $\ddot{\boldsymbol{X}}$ are

vectors containing the velocities and accelerations.

The term F_1 represents the energy absorption of a crashworthy seat and depending on the stage of stroke, determines which part of equation 5 is inputted into the $\boldsymbol{F}$ matrix.

2.5 Equations to Represent a Crashworthy Seat

A FLEA device applies a single, fixed, constant load to decelerate the occupant over a defined displacement, known as stroke [1]. Force 1 in Figure 1 is the force control of the crashworthy seat. It has non-linear characteristics and is modelled by three equations to accurately replicate the stages of energy absorption during a crash, 'before stroke', 'during stroke' and if the load is excessive 'bottom-out'.

In this study, the stroke limit force decelerates only the effective occupant mass and the stroking load is designed for a 50th percentile occupant at 13.2 kN. Once the stroking load is reached, the load remains at 13.2 kN until the stroking length is exhausted or the occupant has returned to zero velocity. If the occupant has not returned to zero before the stroking length is reached, then the seat will bottom-out. In this study, it is assumed that the stiffness of the seat will increase by a factor of four. The force/displacement curve for the crashworthy seat is illustrated in Figure 2. The FLEA device is represented by:

$$\begin{Bmatrix} F_1 = k_1 x_1 & x_1 < l_i \quad \text{Pre Stroke} \\ F_1 = F_s & l_i \le x_1 \le l_s \quad \text{Stroke} \\ F_1 = 4k_1(x_1 - l_s) & x_1 > l_s \quad \text{Bottom out} \end{Bmatrix} \quad (5)$$

where x_1 is the displacement of the seat, l_i is the displacement at which the stroking load is reached at 217 mm and l_s is the stroking length of 370 mm and is the average stroking length from two drop tests of a UH-60 crew seat [6].

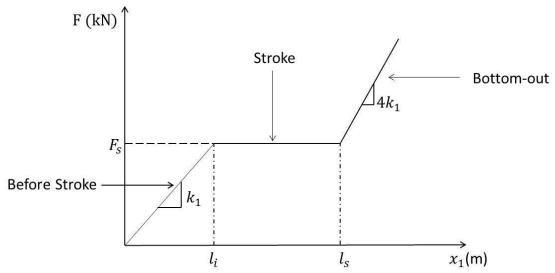

Figure. 2 Force by displacement curve of a typical crashworthy seat

2.6 Loading Conditions

The loading condition placed on the occupant/seat model is an initial impact velocity of 10.2 m/s. This is considered the allowable initial impact velocity for the occupant without equipment. This velocity is deemed a suitable value to represent a vertical helicopter crash.

To solve the EQM a time domain analysis was used, which concerns the real-time results of the simulation. To achieve real-time results, the fourth-order Runge-Kutta method employed by the ODE45 function in MATLAB is used. This method reduces second order differential equations to first order differential equations.

3 Results

3.1 Model Validation

To verify the established model, the model inputs were adjusted to be identical to the 50th percentile ellipsoid hybrid III ATD with 18 kg equipment mass modelled in MADYMO on a FLEA seat [6]. In that study, the deceleration of the cabin floor used a standard military deceleration profile from Military-Standard-58095A [2]. In the model investigated in current study, the cabin floor is not simulated and therefore only an identical velocity to the one used in that study was simulated on the seat and the occupant. The results predicted a maximum lumbar load of 14.5 kN which correlated within 20% of the predicted lumbar load of that study.

3.2 Effect of equipment on initial impact velocity to cause bottom-out

The effect of equipment mass on the minimum initial impact velocity to cause bottom-out is

important to determine an allowable initial impact velocity for each equipment mass condition. This allowable initial impact velocity is the safe velocity preventing bottom-out from occurring.

The seat force is displayed in Fig. 3 for the occupant without equipment and the occupant with the maximum equipment mass and different attachment types. In this figure, the occupant without equipment does not surpass the stroking load and the impact energy is absorbed prior to the seat reaching its full stroking distance, preventing bottom-out. The results in Figure 3 are derived from when the system is placed under an initial impact velocity of 10.2 m/s. An occupant without equipment has an allowable or safe impact velocity of 10.2 m/s. As equipment mass is added and increased, the seat is no longer able to absorb all the impact energy prior to stroke finishing and therefore, bottom-out occurs. This is illustrated in Figure 3. Consequently, if bottom-out occurs, at a certain impact velocity, then this is not a safe or allowable impact velocity. If the seat is able to absorb all the impact energy, at an arbitrary initial impact velocity, then it is a safe impact velocity.

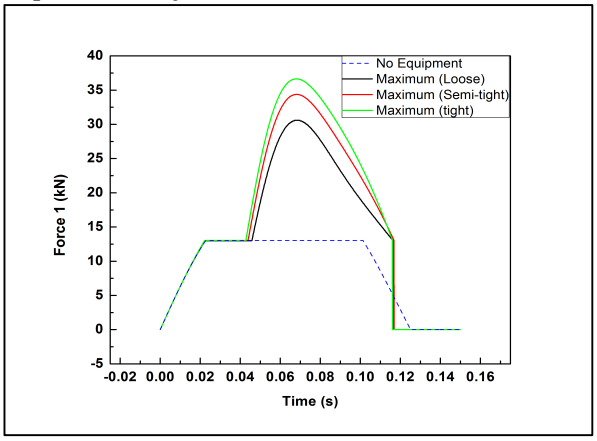

Figure. 3 Variation of predicted seat force (Force 1) during the crash at different equipment attachment conditions, compared with the case without equipment

Table 4 indicates the minimum initial impact velocity at different equipment masses and attachment types to cause bottom-out. The initial impact velocity was varied by 0.1 m/s from 7 m/s to 10.2 m/s and the simulation was conducted to determine the minimum initial impact velocity to cause bottom-out for each equipment mass condition. Any initial impact velocity below these velocities in table 4 for each condition indicates a safe velocity and the seat will be able to absorb the total impact energy regardless of the equipment mass. As the equipment mass increases and the attachments become tighter, the initial impact velocity to cause bottom-out reduces. Without equipment mass, the seat is able to withstand a higher impact velocity, whereas with the highest equipment mass tightly attached, the seats ability to absorb the total impact energy before the stroke ends is considerably diminished and can only withstand an impact velocity of 7.4 m/s. Therefore the velocity the seat is able to withstand reduces by 2.8 m/s, or 28%. At impact velocities below 7.4 m/s with the maximum equipment mass investigated tightly attached the occupant will not experience bottom-out.

Table 4: Effect of equipment mass and attachment type on minimum impact velocity needed to cause bottom-out

Minimum Impact Velocity to Cause Bottom-out (m/s)				
Attachment Type	Low [10,10,0.5]	Medium [20,20,1]	High [30,30,1.5]	Maximum [40,40,2]
Loose	9.6	9	8.5	8.2
Semi-tight	9.7	8.7	8.1	7.5
Tight	9.5	8.7	7.8	7.4

3.3 Force on the bottom of the lower torso

The force on the bottom of the lower torso has the same characteristics as the force limiting mechanism of the seat. This force is imparted on the lower side of the torso and allows the prediction of injury in the lower lumbar area. When the occupant is not wearing equipment, the load is controlled at the stroking load and bottom-out does not occur. As the equipment increases, this load increases, with a maximum load increase of 182%. To investigate the effects of individual equipment locations, equipment masses were isolated and combined. The head equipment mass was found to be inconsequential on this load as a result of the distance between the head and the pelvis and the negligible mass of the head equipment mass.

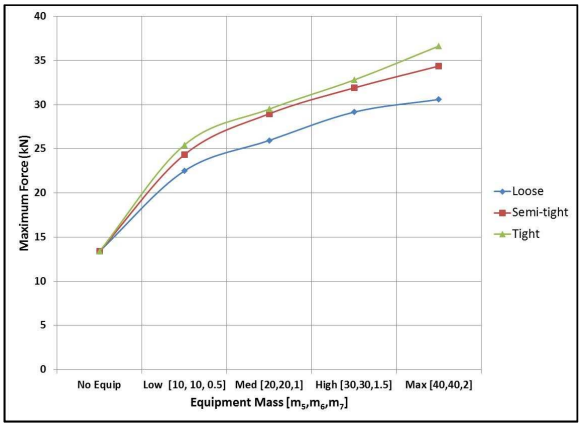

Figure. 4: Maximum Force on the bottom of the torso with different equipment masses and different attachment types

3.4 Force on top of the lower torso

The force on top of the hip is represented by force 2 in Figure 1. Force 2 is a combination of the force from the viscera and the upper torso and contact force from the equipment and is measured to calculate the load on the top of the lower torso mass body. Figure 5 illustrates the force on top of the lower torso mass with increasing equipment mass with different attachment types. With increasing equipment mass and attachment type, a 321% maximum increase in force is measured. Furthermore, the head equipment has a minimal effect on the force on the top of the lower torso.

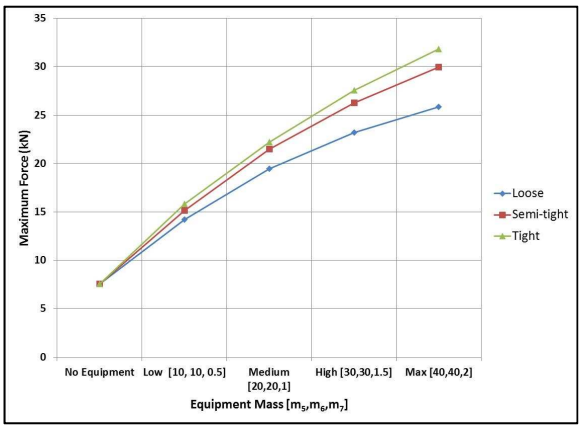

Figure. 5: Maximum Force on the top of the lower torso with different equipment masses and attachment types

3.5 Dynamic Response Index

The dynamic response index (DRI) measures the likelihood of spinal injury in seat ejections; however, it can also be applied to impact cases. A DRI above 17.7 correlates with a 10% chance of spinal injury and is the threshold for military certification [10]. The DRI is calculated by:

$$DRI = \frac{\omega_n^2}{g} X \qquad (6)$$

where ω_n^2 is 52.9 based on experimental tests of U.S. Military Airforce [10], g is acceleration due to gravity and X is the maximum displacement between m_2 and m_1.

Figure 6 illustrates the DRI with increasing equipment mass and different attachment types. Without equipment, the model registers a DRI of 12 corresponding to less than 0.2% probability of spinal injury. The maximum DRI measured is 33, which corresponds to more than a 50% chance of spinal injury. When only upper torso equipment mass is worn, a DRI value of 32 is measured, indicating, the major effect upper torso equipment mass has on this injury criteria. This is to be expected, as the displacement of the two mass bodies increase with equipment mass.

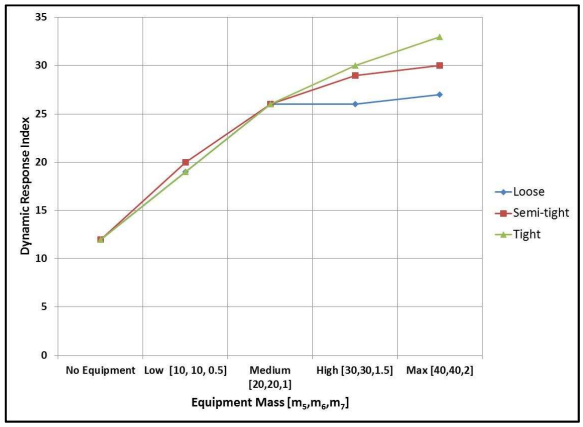

Figure. 6: Dynamic Response Index with different equipment masses and attachment types

3.6 Force on the Upper Torso

The force on top of the upper torso is represented by Force 3 in Fig. 1. Fig. 7 illustrates the force on the upper torso with increasing equipment mass, with different attachment types. As for the other locations measured, the force on top of the upper torso increases with increasing equipment mass. When examining injury, the criteria used for chest or upper torso injury is acceleration of the

chest. A limit of 60 g is considered the humanly tolerable limit [11]. The results show that the acceleration of the upper torso does not pass this limit until the maximum equipment mass is placed semi-tightly at the upper torso. In military operations, a large amount of the equipment mass is located at the upper torso region, and this equipment mass can exceed 40 kg in this region.

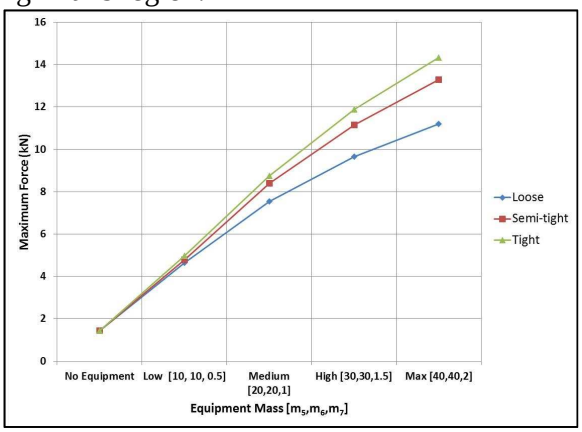

Figure 7: Maximum force on the upper torso with different equipment masses and attachment types

3.7 Force on the Head

The force on top of the head is represented by Force 4 in Fig. 1. Fig. 8 demonstrates that increasing the equipment mass increases the force on the head resulting from the head equipment mass. This force is a contact force from the head equipment mass, so the head equipment mass has the greatest effect. When the occupant is wearing upper torso mass, the accelerations of the head decrease causing m_3 to attain more inertia and therefore its accelerations are reduced. Consequently, when only the head equipment is modelled, the force on the head is greater causing a 36% increase in force on the head than the combination of upper torso and head equipment. The force on the head is substantially affected by the head equipment mass.

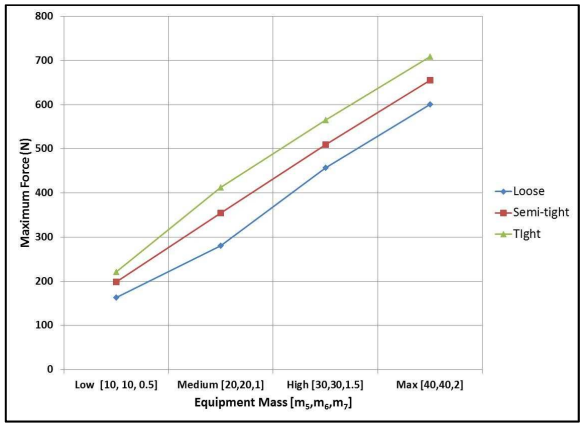

Figure. 8: Maximum Force from the head equipment mass on the head with different equipment masses and attachment types

3.8 Investigating attachment types

The tight equipment attachment provides the greatest force because the high stiffness coefficient causes the loading path of the equipment to be the same as the loading path of the occupant. It is assumed in military operations, that the tighter the equipment is attached to the occupant, the greater chance the load will follow the loading path of the occupant. Consequently, if the same simulation were to be conducted in three dimensions, the loose equipment attachment would demonstrate higher loads in the loading paths in the x and y directions as well as z. The analysis demonstrates that loose attachment would be most beneficial to reduce the force on the occupant; however, it is unrealistic to have all the equipment loosely attached, as the equipment would flail in the cabin. Loosely attached equipment may increase the chances of contact injury and create loads in different loading paths. This was not investigated in this paper.

4 Conclusions

This study used a lumped parameter model to investigate the effects of equipment mass on an occupant seated on a crashworthy seat in a helicopter crash and has provided reasonable results in comparison to a study completed in the literature. The following are the three major conclusions of the study:

1. Tight attachment provides the greatest force at all locations as a consequence of the

loading path following the occupants loading path.
2. Increasing equipment mass and attachment type leads to decrease of the minimum initial impact velocity needed to cause bottom-out to occur.
3. Increasing equipment mass increases the forces at all locations.

A simplified solution to the problems associated with equipment mass increasing the forces on the occupant and potential injury is to remove all military gear on the occupant, however, from an operational position, this is not practical as military personnel are required to wear certain items to protect them in tactical and combat missions.

The method developed and presented was ideal to investigate the effect of equipment mass on occupant forces during a purely vertical crash. Further studies could be completed to investigate alternate equipment loading paths by using a 3 dimensional model. Furthermore, determining the effects on mass-distribution on these forces will help to develop a better method to place the equipment over the body.

Acknowledgement

This work was undertaken as part of Systems for Crashworthiness research project of the CRC-ACS, established and supported under the Australian Government's Cooperative Research Centres Program.

References

[1] Desjardins S.P. The evolution of energy absorption systems for crashworthy helicopter seats. *Journal of the American Helicopter Society*, Vol.1, No.1, pp 150-163, 2006

[2] MIL-S-58095A.Seat system: crash resistant, non-ejection, aircrew general specification for. Department of Defense, Washington DC 1986.

[3] Coltman, J.W. Rotorcraft crashworthy airframe and fuel system technology development program. *Report DOT/FAA/CT-19/7*, Federal Aviation Administration, Washington DC, 1994

[4] Wan Y and Schimmels J.M. A simple model that captures the essential dynamics of a seated human exposed to whole body vibration. *Advances in Bioengineering, ASME, BED* 31, pp 333-33, 1995

[5] Liang C.C and Chiang C.F. A study on biodynamic models of seated human subjects exposed to vertical vibration. *International Journal of Industrial Ergonomics*, Vol. 36, pp 869-890, 2006

[6] Richards M and Sieveka E. The effects of body-borne equipment weight on ATD lumbar loads measured during crashworthy seat vertical dynamic tests. *American Helicopter Society 67 Annual Forum*, Virginia Beach, VA, pp 1-16, 2011

[7] Payne P.R and Band, E.G. A four-degree-of-freedom lumped parameter model of the seated human body. *Aerospace Medical Research laboratory*, 1971

[8] Rao S.S. *Mechanical Vibrations.* SI Edition, Singapore. 1, 2005

[9] Mills N. Polymer foams handbook – Engineering and biomechanics applications and design guide. Elsevier Jordan Hill, Oxford 2007.

[10] Payne P.R and Stech, E.L. Dynamic models of the human body. *Aerospace Medical Research Laboratory*, 1969

[11] Mertz H.J. Injury assessment values used to evaluate hybrid III response measurements. NIHTSA Docket 74-14 Notice 32, Enclosure 2 of the attachment 1 of Part III of General Motors Submission USG 2284 March 22, 19840

8 Contact Author Email Address

mailto:Daniel.aggromito@monash.edu

Copyright Statement